CUDC-305, a Novel Synthetic HSP90 Inhibitor with Unique Pharmacologic Properties for Cancer Therapy

Rudi Bao, Cheng-Jung Lai, Hui Qu, Dagong Wang, Ling Yin, Brian Zifcak, Ruzanna Atoyan, Jing Wang, Maria Samson, Jeffrey Forrester, Steven DellaRocca, Guang-Xin Xu, Xu Tao, Hai-Xiao Zhai, Xiong Cai, and Changgeng Qian

Abstract

Purpose: We designed and synthesized CUDC-305, an HSP90 inhibitor of the novel imidazopyridine class. Here, we report its unique pharmacologic properties and antitumor activities in a variety of tumor types.

Experimental Design: The potency of the compound was analyzed by fluorescence polarization competition binding assay. Its antiproliferative activities were assessed in 40 human cancer cell lines. Its pharmacologic properties and antitumor activities were evaluated in a variety of tumor xenograft models.

Results: CUDC-305 shows high affinity for HSP90α/β (IC_{50}, ~100 nmol/L) and HSP90 complex derived from cancer cells (IC_{50}, 48.8 nmol/L). It displays potent antiproliferative activity against a broad range of cancer cell lines (mean IC_{50}, 220 nmol/L). CUDC-305 exhibits high oral bioavailability (96.0%) and selective retention in tumor (half-life, 20.4 hours) compared with normal tissues. Furthermore, CUDC-305 can cross blood-brain barrier and reach therapeutic levels in brain tissue. CUDC-305 exhibits dose-dependent antitumor activity in an s.c. xenograft model of U87MG glioblastoma and significantly prolongs animal survival in U87MG orthotopic model. CUDC-305 also displays potent antitumor activity in animal models of erlotinib-resistant non–small cell lung cancer and induces tumor regression in animal models of MDA-MB-468 breast cancer and MV4-11 acute myelogenous leukemia. Correlating with its efficacy in these various tumor models, CUDC-305 robustly inhibits multiple signaling pathways, including PI3K/AKT and RAF/MEK/ERK, and induces apoptosis. In combination studies, CUDC-305 enhances the antitumor activity of standard-of-care agents in breast and colorectal tumor models.

Conclusion: CUDC-305 is a promising drug candidate for the treatment of a variety of cancers, including brain malignancies.

Recent advances in understanding the molecular biology of cancer have resulted in the development of drugs that target known molecular pathways (1). For a limited number of cancer subtypes, these drugs exploit the dependence of the tumor on dysregulated signaling pathways to achieve therapeutic selectivity for cancer over normal cells. Molecularly targeted agents that have been approved for clinical use include imatinib (Gleevec), a small-molecule inhibitor of BCR/ABL kinase in chronic myelogenous leukemia; trastuzumab (Herceptin), an antibody against ERBB2 (HER2) in breast cancer; bevacizumab (Avastin), an antibody against vascular endothelial growth factor in solid tumors; and erlotinib (Tarceva), a small-molecule inhibitor of epidermal growth factor receptor (EGFR) in non–small cell lung cancer (NSCLC; refs. 2–5).

However, it has been increasingly recognized that, in each individual tumor, there are a large number of mutated genes that disrupt multiple pathways, which normally exhibit extensive biological cross-talk and redundancy (6). Therefore, interfering with a single target and/or pathway may not abrogate the malignant phenotype of most tumors. For example, among the roughly 20% of breast cancer patients with HER2 overexpression, only one third respond to trastuzumab treatment. The remaining two thirds of patients fail to respond, which is likely due to other distinct molecular abnormalities within their tumors, such as activation of the insulin-like growth factor signaling pathway (7). Furthermore, resistance to molecularly targeted agents can develop through secondary target gene mutation or compensatory activation of alternative pathways, so-called "oncogenic switching."

This problem is exemplified by erlotinib, an EGFR inhibitor that has been approved for use in NSCLC. An activating mutation in EGFR (exon 19 deletions or exon 21 point mutation

Authors' Affiliation: Curis, Inc., Cambridge, Massachusetts
Received 1/21/09; revised 3/16/09; accepted 3/19/09; published OnlineFirst 6/9/09. The costs of publication of this article were defrayed in part by the payment of page charges. This article must therefore be hereby marked *advertisement* in accordance with 18 U.S.C. Section 1734 solely to indicate this fact.
Note: R. Bao and C. Lai contributed equally to this work.
Requests for reprints: Rudi Bao, Oncology, Curis, Inc., 45 Moulton Street, Cambridge, MA 02138. Phone: 617-503-6540; Fax: 617-503-6501; E-mail: rbao@curis.com.

doi:10.1158/1078-0432.CCR-09-0152

Translational Relevance

CUDC-305 is a novel HSP90 inhibitor of the imidazopyridine class that displays more favorable pharmacologic properties, including high oral bioavailability, sustained tumor retention, blood-brain barrier penetration, and potentially a better therapeutic window, compared with the HSP90 inhibitors currently in clinical development. Most importantly, it displays potent antitumor activity against a variety of tumor types *in vitro* and *in vivo*, including epidermal growth factor receptor inhibitor–resistant, non–small cell lung cancer, glioblastoma, triple-negative breast cancer, and acute myelogenous leukemia. Remarkably, all of these tumors represent crucial unmet medical needs. Mechanistically, CUDC-305 robustly inhibits multiple signaling pathways and induces apoptosis in cancer cells. Taken together, these original findings may have a significant effect on future clinical practice in cancer therapy, particularly in the above-mentioned cancer types.

L858R) renders cancer cells sensitive to the EGFR inhibitor. However, subsequent resistance to erlotinib emerges as a result of an additional EGFR mutation (T790M) or amplification and/or activation of parallel signaling pathways, including ERBB3 (HER3), insulin-like growth factor receptor, and c-MET (8–10). A promising strategy for mitigating such acquired drug resistance is to simultaneously inhibit multiple molecular pathways, either by using several agents in combination or by using a single agent that concurrently blocks multiple targets or pathways.

One approach to inhibiting multiple pathways with one single agent is to target the heat shock protein HSP90. Among the "client proteins" that HSP90 chaperones are many oncogenic proteins, such as the estrogen receptor, androgen receptor, HER2, ERBB1 (EGFR), MEK, c-MET, AKT, MAPK (ERK), CDK, RAF, BCR/ABL, HIF1-α, and hTERT (11). These oncoproteins, ranging from transcription factors and kinases to antiapoptotic molecules, are involved in cancer cell proliferation, survival, invasion, metastasis, and angiogenesis (11). It has been shown that pharmacologic inhibition of HSP90 function can trigger proteasomal degradation of multiple oncoproteins, thereby reducing cancer cell proliferation/survival and tumor angiogenesis and promoting apoptosis (12–14).

The chaperone function of HSP90s is highly dependent on its ATPase activity. HSP90 inhibitors compete with ATP at the NH_2 terminal nucleotide-binding site to neutralize the intrinsic ATPase activity of the protein. In preclinical tumor models, HSP90 inhibitors have been shown to deplete oncoproteins and inhibit tumor growth (15). The most advanced class of HSP90 inhibitors, including tanespimycin and other 17-AAG derivatives, are now in phase II/phase III clinical trials for solid and hematologic malignancies. A combination of tanespimycin and trastuzumab has shown encouraging results in a phase II trial for trastuzumab refractory breast cancer (16). However, significant clinical limitations of these 17-AAG derivatives have been reported, including poor solubility, potential liver toxicity, substrate for the P-glycoprotein multidrug resistance efflux pump, quinine reductase NQO1 dependence, and limited oral bioavailability (17–19).

To overcome the limitations of the 17-AAG class of HSP90 inhibitors, several synthetic HSP90 inhibitors have recently been discovered (20–22) and are now being tested in phase I/phase II clinical trials. Importantly, these synthetic HSP90 inhibitors, including purine (BIIB-021), isoxazole (VER-52296, NVP-AUY922), and indazole (SNX-5422) classes exhibit more favorable pharmacologic properties than the 17-AAG class inhibitors (20–22). Here, we describe CUDC-305, a leading HSP90 inhibitor of the imidazopyridine class. In addition to potent antitumor efficacy against a broad range of cancers in preclinical tumor models, we report that CUDC-305 exhibits enhanced pharmacologic features in several areas, including high oral bioavailability, selectivity, blood-brain barrier penetration, and extended tumor retention.

Materials and Methods

Reagents and chemicals. CUDC-305 and other reference HSP90 inhibitors were synthesized in house. For *in vitro* assays, compounds were dissolved in DMSO as stock and stored at −20°C. For *in vivo* studies, CUDC-305 was formulated in 30% Captisol (Cydex Pharmaceuticals, Inc.) with 2 molar equivalents of HCl. Paclitaxel (Taxol, 6 mg/mL) was purchased from Mayne Pharma, Inc. Camptothecin-11 (20 mg/mL) was purchased from Pfizer, Inc.

All other reagents including culture medium, unless otherwise stated, were purchased from Invitrogen.

Assay for HSP90 binding. COOH terminal His-tagged human HSP90α and HSP90β proteins were expressed in *Escherichia coli*. Fluorescence polarization competition binding assays were done with purified HSP90α or HSP90β and FITC-labeled geldanamycin (InvivoGen) in the presence of different concentrations of test articles. The final reaction contained 10 and 50 nmol/L of labeled geldanamycin and purified HSP90 protein, respectively. The assay buffer contained 20 mmol/L HEPES (pH 7.3), 50 mmol/L KCl, 1 mmol/L DTT, 50 mmol/L $MgCl_2$, 20 mmol/L Na_2MoO_4, and 0.01% NP40 with 0.1 mg/mL bovine γ-globulin. Polarization degree (mP) values were determined using a Synergy II plate reader (BioTek Instruments, Inc.) with background subtraction after 24 h of incubation at 4°C.

For binding assay with HSP90 complex from cancer, cancer cell lines were cultured in flasks. Total protein was extracted with radioimmunoprecipitation assay buffer (Sigma-Aldrich Corp.) following manufacturer's instructions. Fluorescence polarization competition binding assay was done as described above. Final protein concentration was adjusted to achieve the same FITC-geldanamycin binding level as with purified HSP90α or HSP90β without test articles.

Cell growth and viability assay. Human cancer cell lines were purchased from American Type Culture Collection and plated at 5,000 to 10,000 per well in 96-well plates with culture medium, as suggested by the provider. The cells were then incubated with compounds at various concentrations for 120 h. Growth inhibition was assessed by ATP content assay using the Perkin-Elmer ATPlite kit. Briefly, a 25-μL cell lysis solution was added to the 50-μL phenol red–free culture medium per well to lyse cells and stabilize ATP. Then 25-μL substrate solutions were added to the wells, and subsequently, luminescence was measured with a TopCount liquid scintillation analyzer (Perkin-Elmer). Values were expressed as a percentage relative to those obtained in untreated controls. IC_{50} values were calculated using PRISM software (GraphPad Software) with sigmoidal dose-response curve fitting.

Western blot analysis of cells in culture. Cancer cells grown in culture were treated with compounds at 1 μmol/L for 24 h and then harvested in 1× sample loading buffer (Sigma-Aldrich Corp.). Cell lysates were resolved on NuPAGE Novex 4-12% bis-Tris gels (Invitrogen) and then

transferred to nitrocellulose membranes (Bio-Rad Laboratories). The blots were incubated first with a primary antibody overnight at 4°C. Antibodies to detect HSP70, AKT, phosphorylated AKT (p-AKT), c-MET, phosphorylated MET, EGFR, FLT3, phosphorylated FLT3, ERK1/2, phosphorylated ERK1/2 (p-ERK1/2), HER2, phosphorylated HER2, phosphorylated HER3, estrogen receptor α, androgen receptor, CDK4, MEK1, survivin, activated CDC42-associated kinase, signal transducers and activators of transcription 5 (STAT5), cleaved poly(ADP-ribose) polymerase, and c-RAF (1:1,000-2,000) were obtained from Cell Signaling Technology. Antibody against cyclin D1 (1:2,000) was obtained from Santa Cruz Biotechnology. Glyceraldehyde-3-phosphate dehydrogenase (1:30,000; Abcam) or tubulin (1:5,000; Sigma-Aldrich) was used as an internal control for each assay. Membranes were then incubated with an IR-labeled secondary antibody (1:10,000): conjugated IR Dye-800 (Rockland Immunochemicals, Inc.) or conjugated Alexa Fluor-680 (Invitrogen). Membranes were imaged with the Odyssey IR Imaging System (Li-Cor Biotechnology).

Animals and tumor implantation. Female athymic nude (CD-1 nu/nu) or severe combined immunodeficient mice (6-8 wk of age) were obtained from Charles River Laboratories for in-house studies. For efficacy studies conducted in Crown Biosciences, Inc., BALB/c nu/nu mice were used. Animals were housed in ventilated microisolator cages in the animal facilities conditioned at a temperature of 23 ± 1°C, humidity of 50% to 70%, and a 12-h light/12-h dark cycle. The mice were provided with sterile laboratory rodent diet and water *ad libitum*. The animal procedures and protocols were approved by the Institutional Animal Care and Use Committee of Curis and Crown Biosciences, Inc., respectively.

Before tumor implantation, various cancer cell lines of human origin were cultured in the medium suggested by the provider. When cultured cells reached ~70% to 90% confluence. They were harvested by treatment with trypsin-EDTA (0.25% trypsin, 1 mmol/L EDTA). The cell pellet was suspended in HBSS for implantation after medium was removed.

For s.c. tumor implantation, various numbers ($3\text{-}20 \times 10^6$) of cancer cells were injected into the right hind flank region of each mouse. For orthotopic implantation of breast cancer, a small incision (5 mm) was made in the skin over the lateral thorax to expose the mammary fat pad. MDA-MB-468 cancer cells (20×10^6) suspended in 100 μL HBSS were injected into the mammary fat pad. Tumor size was measured with an electronic caliper. The following formula was used to calculate the tumor volume (23):

$$\text{Tumor volume} = (\text{length} \times \text{width}^2)/2.$$

For intracranial implantation into nude mice, a 2- to 3-mm incision was made in the skin along the cranial midline. The injection needle was inserted 2.0 mm to the right and 0.5 mm anterior of the bregma. U87MG tumor cells (6×10^4) were then injected to a depth of 3.5 mm in the right frontal lobe of brain.

Pharmacokinetic studies. Tumor-bearing nude mice were used for pharmacokinetic studies. CUDC-305 formulated in 30% Captisol

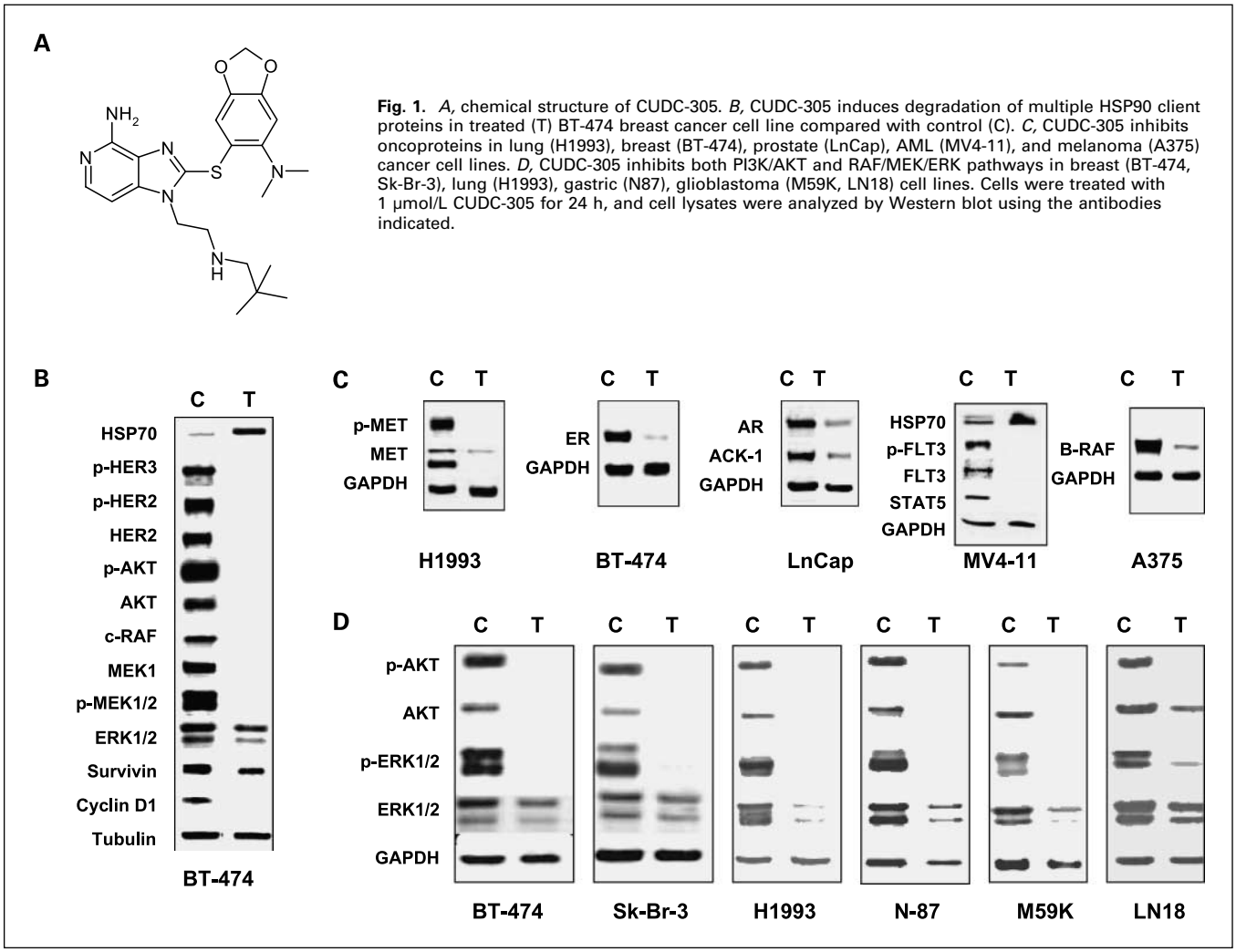

Fig. 1. *A,* chemical structure of CUDC-305. *B,* CUDC-305 induces degradation of multiple HSP90 client proteins in treated (T) BT-474 breast cancer cell line compared with control (C). *C,* CUDC-305 inhibits oncoproteins in lung (H1993), breast (BT-474), prostate (LnCap), AML (MV4-11), and melanoma (A375) cancer cell lines. *D,* CUDC-305 inhibits both PI3K/AKT and RAF/MEK/ERK pathways in breast (BT-474, Sk-Br-3), lung (H1993), gastric (N87), glioblastoma (M59K, LN18) cell lines. Cells were treated with 1 μmol/L CUDC-305 for 24 h, and cell lysates were analyzed by Western blot using the antibodies indicated.

as a clear solution (20 mg/mL) was injected i.v. through tail vein (10 mg/kg) or orally via gavage (30 or 160 mg/kg) to each animal based on its body weight. At various time points after compound administration, three mice per time point were euthanized with CO_2, and blood and tissues were collected. Blood was collected into tubes containing sodium heparin. The plasma was separated via centrifugation. Plasma and tissues were stored at −80°C for later analysis. Analyte in storage condition was confirmed to be stable.

To prepare plasma sample for liquid chromatographic mass spectrometric (LC-MS/MS) analysis, 50 μL plasma added to 5 μL internal standard were mixed with 150 μL acetonitrile. The samples were vortexed and then centrifuged for 5 min at 1,000 × *g*. The supernatant was collected for LC-MS/MS analysis.

To prepare tissue samples, including tumors for LC-MS/MS analysis, tissues were homogenized in 150 μL water with 5 μL internal standard in acetonitrile. The homogenates were extracted thrice with 1.2 mL ethyl acetate. After evaporation, the residual was reconstituted in 0.1 mL acetonitrile for LC-MS/MS analysis.

A PE Sciex API-3000 LC-MS/MS system (Applied Biosystems, Inc.) was used to analyze compound concentrations in plasma and various tissues. Five microliters of each sample were injected; the flow rate was 200 μL/min. The limit of detection of analyte was 1 ng/mL in plasma and 2 ng/g in tissues. The assay was linear in the concentration range of 1 to 2,000 ng/mL in plasma and 4 to 4,000 ng/g in tissues. The recovery rate over above concentration range was >85.6% in plasma and >81.2% in tissues, respectively.

Pharmacodynamic studies. A single-dose pharmacodynamic (PD) study was routinely conducted to evaluate the biological effects of the compound at molecular levels in established tumor model before efficacy study was initiated. For single-dose PD study, three mice per time point were sacrificed and tumors were collected for Western blot analysis after a single oral dosing of CUDC-305. In the case of efficacy study in U87MG s.c. tumor model, tumors were also collected at the end of the efficacy study for Western blot and immunohistochemical analyses to assess the correlation between PD and efficacy results.

For Western blot analysis of tumors, tumor tissues were collected and placed in dry ice until transferred to −80°C. Protein was extracted using Tissuelyser (Qiagen) and T-PER tissue protein extraction reagents plus Halt protease/phosphatase inhibitor cocktail (Thermo Fisher Scientific) following manufacturers' instructions. Protein (30 μg) was routinely used for Western blot analysis as described above.

For immunohistochemical analysis, tumor tissues were collected, then fixed in neutral buffered formalin overnight at room temperature, and then embedded in paraffin. For Ki-67 staining, tumor sections were first incubated with mouse monoclonal Ki-67 antibody (1:200; mib-1; Dako), then with horseradish peroxidase–labeled secondary antibody-polymer complex (Envision-HRP; Dako). For CD34 staining, tumor sections were first incubated with rat monoclonal CD34 antibody (1:200; Santa Cruz Biotechnology), then with biotin-labeled goat anti-rat antibody, and finally with peroxidase-conjugated streptavidin (BioGenex). Diaminobenzidine solution (Dako) was applied to the section for color development. The sections were counterstained with hematoxylin. A Nikon E-800 microscope coupled with an imaging system (Bioquant Life Science, V8) was used for image acquisition (100 × amplification).

Efficacy studies in animal models of cancers. When tumors were established after implantation, animals with proper tumor size were randomly assigned into different groups. CUDC-305 was formulated in 30% Captisol and delivered by oral gavage based on the body weight of each individual animal. The control group was treated with vehicle (30% Captisol) using the same dosing paradigm. In combination studies, paclitaxel or camptothecin-11 was diluted in 0.9% normal saline and injected i.p. twice weekly.

During study period, tumors were measured with an electronic caliper and body weights were measured with a scale twice a week. The last tumor measurement was used to calculate the tumor volume change ratio (%T/C = 100 × $\Delta T/\Delta C$), a standard metric developed by National Cancer Institute for evaluation of antitumor activity of investigational compounds in animal models (24).

For survival studies in intracranial tumor models, treatment with CUDC-305 started 5 d after tumor implantation. Mice were monitored daily for general health. Animals were sacrificed when moribund clinical signs appeared, such as progressive weight loss, cachexia, hunchback posture, paralysis, and obvious abnormal behavior.

Statistical analysis. Two-way ANOVA was used to calculate the significance of difference of tumor size between different groups. The log-rank (Mantel-Cox) test was used for statistical analysis of animal survival.

Results

CUDC-305 is a potent and novel HSP90 inhibitor. We designed and synthesized CUDC-305, which belongs to the novel imidazopyridine class of HSP90 inhibitors (Fig. 1A; ref. 25). In a competitive assay with geldanamycin to measure the interaction with the HSP90 NH_2 terminal ATP binding domain, CUDC-305 displayed a binding affinity for purified HSP90α protein (IC_{50}, 100.0 nmol/L), which is similar to those of HSP90 inhibitors SNX-2112 (active metabolite of clinical candidate SNX-5422) and BIIB-021 (IC_{50}, 81.0 and 52.0 nmol/L, respectively). CUDC-305 also showed comparable affinities (IC_{50}, 103.0 nmol/L) for purified HSP90β protein (93.0 and 54.5 nmol/L for SNX 2112 and BIIB-021, respectively). Using cell extracts prepared from 5 cancer cell lines, we observed that CUDC-305 bind to the tumor HSP90 complex (mean IC_{50}, 48.8 nmol/L) with a similar affinity relative to the reference compound SNX-2112 (mean IC_{50}, 56.8 nmol/L).

***CUDC-305 induces degradation of multiple oncoproteins* in vitro.** The HSP90 chaperone complex regulates many client proteins that play key roles in tumor formation and progression. Therefore, we next examined whether HSP90 inhibition by CUDC-305 can induce degradation of these oncoproteins. In the HER2 overexpressing BT-474 breast cancer cells, CUDC-305 treatment reduced the levels of HER2/phosphorylated HER2 and phosphorylated HER3 and suppressed downstream AKT and RAF/MEK/ERK signaling. CUDC-305 also down-regulated survivin and cyclin D1, further supporting its proapoptotic and antiproliferative roles in cancer cells (Fig. 1B). The reduction of HSP90 client proteins was concurrent with an increase of HSP70, a marker of HSP90 inhibition. These results suggest that CUDC-305 specifically targets HSP90 and suppresses receptor tyrosine kinase signaling.

We further showed that CUDC-305 can effectively decrease the levels of specific oncogenic proteins in different cancer types. As shown in Fig. 1C, a reduction in the levels of c-MET was observed after CUDC-305 treatment in H1993 NSCLC cell line, which is resistant to erlotinib due to *MET* amplification. Moreover, in the BT-474 breast cancer cell line, we observed a reduction in the levels of the estrogen receptor, a potential signaling mechanism to overcome HER2 inhibition (26). Similarly, in the LnCap prostate cancer cell line, we noticed a decrease in the levels of the mutated androgen receptor and activated CDC42-associated kinase, which potentially cause hormone refractory prostate cancer. *FLT-3* mutation with internal tandem duplication and *B-RAF* mutation (*V600E*), which occurs in acute myelogenous leukemia (AML) and melanoma, respectively, were both inhibited by CUDC-305 treatment (Fig. 1C). Importantly, CUDC-305 was able to suppress two major signaling cascades, PI3K/AKT and RAF/MEK/ERK, which are essential for cancer cell proliferation and survival in different cancer types (Fig. 1D). Taken together,

Table 1. Antiproliferative activity of CUDC-305 in 40 human cancer cell lines

Cancer type	Cell line	IC_{50} (μmol/L)
NSCLC	A549	0.70
NSCLC	H1975	0.14
NSCLC	H292	0.22
NSCLC	H2122	0.12
NSCLC	Calu-6	0.15
NSCLC	H1993	0.12
NSCLC	H460	0.16
NSCLC	H1703	0.16
NSCLC	H358	0.20
Glioblastoma	M59K	0.67
Glioblastoma	U118MG	0.20
Glioblastoma	LN18	0.17
Glioblastoma	U87MG	0.46
Glioblastoma	U251	0.29
Hepatic cancer	HepG2	0.13
Hepatic cancer	Hep3B2	0.36
Gastric cancer	N87	0.04
Colon cancer	HCT-116	0.81
Colon cancer	WiDr	0.16
Breast cancer	MDA-MB-468	0.14
Breast cancer	BT-474	0.14
Breast cancer	SkBr3	0.37
Ovarian cancer	OVCAR3	0.15
Ovarian cancer	SKOV3	0.30
Mesotheloma	MSTO-211h	0.42
Pancreatic cancer	HPAC1	0.50
Pancreatic cancer	BxPC3	0.52
Prostate cancer	LnCap	0.40
Prostate cancer	PC-3	0.30
Renal cancer	Caki	0.90
Sarcoma	SK-ES-1	0.07
Sarcoma	Saos-2	0.22
Sarcoma	MNNG HDS	0.44
Melanoma	A375	0.21
AML	HL-60	0.18
AML	MV4-11	0.10
CTCL	MJ	0.13
NHL	Pfeiffer	0.57
NHL	OPM-2	0.04
Multiple myeloma	RPMI8226	0.32

Abbreviations: CTCL, cutaneous T-cell lymphoma; NHL, non–Hodgkins lymphoma.

our results show that CUDC-305 is able to deplete essential regulators of cancer cell proliferation and survival.

***CUDC-305 inhibits cancer cell proliferation* in vitro.** To further confirm its anticancer activity, we tested the growth inhibitory effects of CUDC-305 against a total of 40 human cancer cell lines, including 34 solid and 6 hematologic tumor–derived lines (Table 1). CUDC-305 inhibited the proliferation of these cancer cell lines with an IC_{50}, ranging from 40 to 900 nmol/L (mean IC_{50}, 220 nmol/L).

Interestingly, we noticed that cancer cell lines with *HER2* overexpression and/or amplification, such as BT-474 (breast cancer; IC_{50}, 140 nmol/L) and N87 (gastric cancer; IC_{50}, 40 nmol/L), were quite sensitive to CUDC-305, as was an AML cell line, MV4-11, carrying a *FLT3* internal tandem duplication mutation (IC_{50}, 100 nmol/L). These observations are consistent with the notion that CUDC-305 can down-regulate key mediators of receptor tyrosine kinase signaling and provide further support for HSP90 inhibition as an important therapeutic approach to receptor tyrosine kinase–dependent tumors.

Notably, among the NSCLC cell lines we tested, CUDC-305 was able to effectively inhibit the proliferation of cells that are resistant to conventional EFGR inhibitors, including H1975 (*EGFR* secondary mutation, *T790M*), Calu-6 (*K-ras* mutation), H1993 (*c-MET* amplification), and H460 (*K-ras* and *PI3K* mutations). These results strongly suggest that HSP90 inhibition is an effective therapeutic strategy to overcome resistance to traditional receptor tyrosine kinase inhibitors.

Estrogen receptor, progesterone receptor, and HER2 triple-negative breast cancer tumors have an unfavorable prognosis, and chemotherapy is currently the sole option for treatment. Notably, CUDC-305 inhibited the proliferation of MDA-MB-468, a triple-negative breast cancer cell line, with a low IC_{50}, of 140 nmol/L. This result suggests that, due to its effects on many oncogenic proteins, our HSP90 inhibitor may bring potential therapeutic benefits to important areas with unmet medical needs.

CUDC-305 exhibits favorable pharmacokinetic profiles in tumor-bearing nude mice. The oral bioavailability in mice was determined by calculating percentage of plasma area under concentration-time curve (AUC) after oral administration versus plasma AUC achieved after i.v. administration of compound. The AUC values after oral (30 mg/kg) and i.v. (10 mg/kg) administration of CUDC-305 were 6.2 and 2.2 μmol/L h, respectively. Hence, oral bioavailability (F) of CUDC-305 in mice is 96.0%. In addition, CUDC-305 tends to be retained in tumor longer than in normal tissues after oral administration. As shown in Fig. 2A, CUDC-305 dosed orally at 30 mg/kg exhibited a maximum concentration (C_{max}) of 1.3 μmol/L and a half-life of 7.8 hours in plasma, yet it reached a much higher concentration (C_{max}, 4.7μmol/L) with a much longer half-life ($T_{1/2}$, 20.4 hours) in tumors. The AUC values for tumor and plasma were 114.9 and 6.2 μmol/L hours, respectively, with a ratio of 18.5:1, indicating a very high and durable distribution of CUDC-305 in tumor tissue after oral administration. Furthermore, CUDC-305 displayed a much longer half-life in tumor (20.4 hours) than in normal tissues (2-7 hours). For example, CUDC-305 was cleared quickly from liver tissue with a half-life of only 2.6 hours, although it reached a very high concentration after oral administration (Fig. 2A). Of particular note, CUDC-305 exhibited a therapeutic exposure in brain tissue (C_{max}, 3.1 μmol/L; AUC, 23.7 μmol/L h; AUC brain/AUC plasma, 3.8:1), with a half-life of 4.0 hours (Fig. 2A). This result indicates that CUDC-305 can penetrate blood-brain barrier, which may be therapeutically beneficial in the clinic.

When CUDC-305 was dosed orally at its maximum tolerated dose (160 mg/kg in nude mice), a roughly dose-proportional exposure in plasma was achieved (AUC, 42.6 μmol/L h). However, higher than the dose-proportional exposure (AUC, 1124.4 μmol/L h) was observed in tumor tissues. Even at 48 hours, a high-level (9.4 μmol/L) CUDC-305 could be detected in tumor tissue, whereas compound concentrations in plasma and normal organs were negligible (data not shown).

CUDC-305 induces degradation of HSP90 client proteins, inhibits tumor growth, and prolongs survival in various animal models of U87MG glioblastoma. Given the therapeutically relevant exposure of CUDC-305 in brain tissue, we decided to test the efficacy of the compound in the U87MG glioblastoma tumor models. A single-dose PD study was first conducted to evaluate

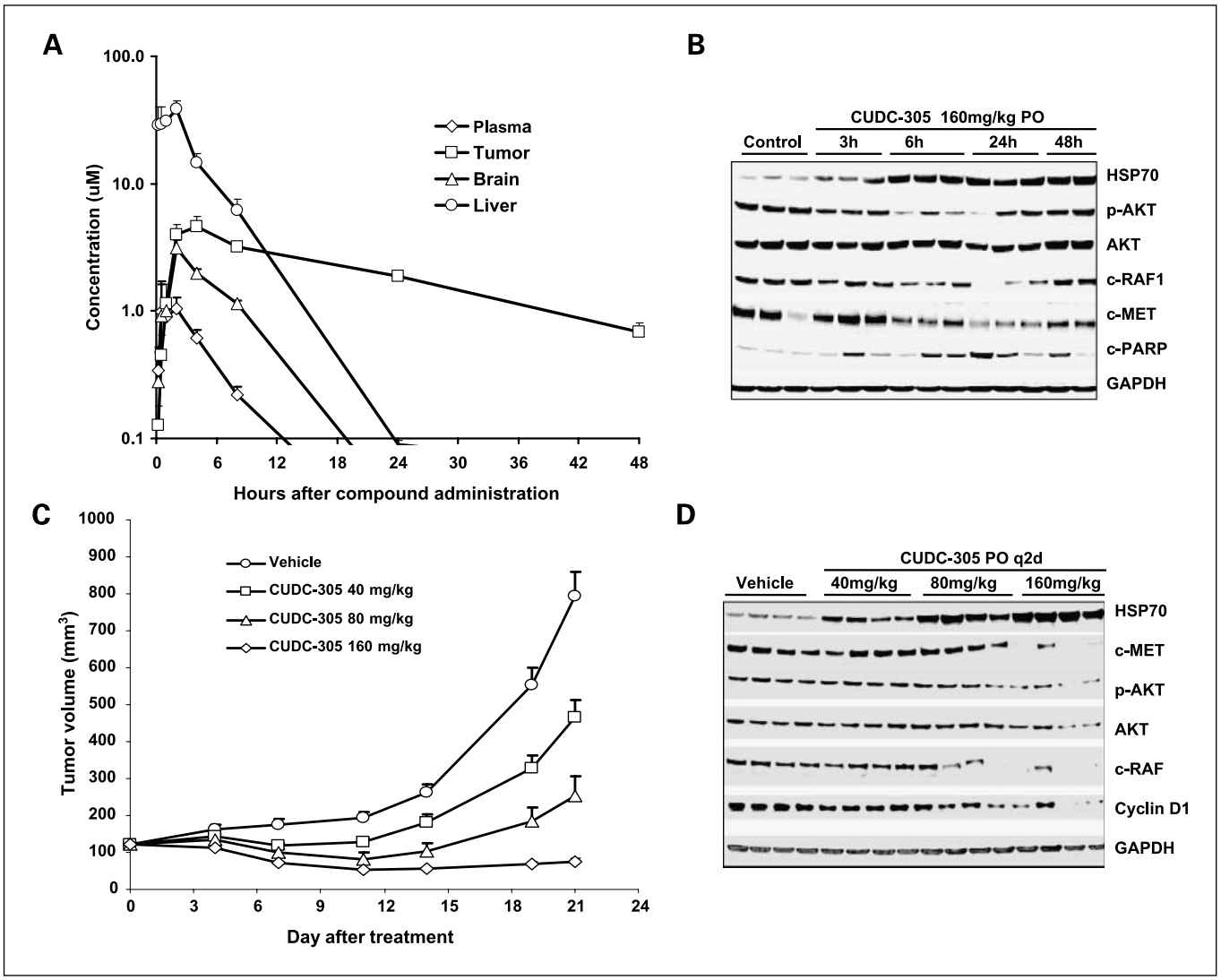

Fig. 2. *A,* CUDC-305 concentration over time curves in plasma, tumor, brain, and liver tissues after single oral dosing of CUDC-305 at 30 mg/kg. CUDC-305 formulated in 30% Captisol was injected orally at 30 mg/kg to each animal based on its body weight. Plasma, normal tissues, and tumors were collected at various time points ($n = 3$) and analyzed with LC-MS/MS. Selective compound retention in tumor and therapeutic exposure in brain were observed. *B,* PD study after single oral dosing of CUDC-305 in U87MG s.c. tumors. CUDC-305 at 160 mg/kg was dosed once to each animal when tumors were established. Tumors were collected at various time points ($n = 3$), homogenized, and analyzed by Western blot using antibodies as indicated. Potent induction of HSP70, inhibition of multiple HSP90 client proteins, and induction of apoptosis were observed. *C,* efficacy study of CUDC-305 in the U87MG s.c. tumor model ($n = 8$). Cells (4×10^6) were implanted s.c. into nude mice. When tumors reached an average of 122 mm^3, mice were treated with vehicle control or CUDC-305 at 40, 80, or 160 mg/kg, orally, q2d for 3 wk. Dose-dependent antitumor effects were observed ($P < 0.001$). *D,* PD result analyzed by Western blot in U87MG s.c. tumors treated with CUDC-305 for 3 wk compared with vehicle control ($n = 4$). After a dosing period of 21 d, mice were sacrificed and 4 tumors from each group were collected for Western blot analysis using antibodies as indicated. Results showed dose-dependent inhibition of multiple HSP90 client proteins, correlating with efficacy results.

the duration of its biological effects in tumor xenografts implanted s.c. After a single oral dosing of CUDC-305 at 160 mg/kg, U87MG tumors were collected at various time points over a 48-hour period and subjected to Western blot analysis. As shown in Fig. 2B, HSP70 was induced from 3 to 48 hours after compound administration, correlating with our earlier findings of extended tumor exposure (9.4 μmol/L at 48 hours, 20-fold above IC_{50} in U87MG cells) after a single oral dosing of CUDC-305 at 160 mg/kg. Therefore, an every-other-day (q2d) dosing regimen was adopted for most efficacy studies. HSP90 client proteins, including p-AKT, and c-RAF were shown to be down-regulated, along with the induction of apoptosis as measured by poly(ADP-ribose) polymerase cleavage (Fig. 2B). Note that although minimal or no inhibition was observed for c-MET or total AKT in this single-dose PD study, inhibition of these HSP90 client proteins was achieved after multiple oral doses, as shown in our subsequent efficacy-PD study in the same tumor model.

Next, we evaluated the antitumor efficacy of the compound in the same U87MG s.c. tumor model. CUDC-305 was delivered orally at three dosage levels (40, 80, or 160 mg/kg, orally, q2d) when tumors reached an average volume of 122 mm^3. During treatment period, tumor volume and body weight were measured twice weekly to determine antitumor activity

and toxicity of compound. In addition, tumors from each group were collected at the end of the efficacy study for both Western blot and immunohistochemical analyses.

As shown in Fig. 2C, CUDC-305 displayed dose-dependent inhibition of tumor growth in the U87MG s.c. tumor model. The T/C values were 51.1% ($P < 0.001$) for the 40 mg/kg group and 19.6% ($P < 0.001$) for the 80 mg/kg group. Tumor regression was observed in the group treated at 160 mg/kg (regression of 37.9%, $P < 0.001$). No loss of body weight or other side effects were observed in any of the treatment groups.

Four tumors from each treatment group were collected at the end of the efficacy study and subjected to Western blot analysis. HSP70 was strongly induced in a dose-dependent manner (Fig. 2D), in agreement with the efficacy results (Fig. 2C). HSP90 client proteins, including c-MET, p-AKT, AKT, c-RAF, and cyclin D1, were potently inhibited in the high-dose group (160 mg/kg). It was noticeable that, in the 2 low-dose groups (40 and 80 mg/kg), minimal inhibition of these client proteins was observed (Fig. 2D). Because all tumors were collected 12 hours after the last dosing, it is possible that lower doses of compounds have resulted in a shorter period of inhibition of these proteins, which could not be captured at a later time point.

Three tumors from each treatment group were also collected at the end of the efficacy study and subjected to immunohistochemical analysis. Cell proliferation, as measured by Ki-67 staining, was inhibited in a dose-dependent manner (Fig. 3A). This result is in accordance with the suppression of cell proliferation and survival pathways by CUDC-305 observed in Western blot analysis (Fig. 2D). Microvessel density, as measured by CD34 staining, showed a dose-dependent reduction (Fig. 3B), suggesting that CUDC-305 has antiangiogenic effects.

To further assess the ability of CUDC-305 to cross blood-brain barrier and inhibit orthotopic tumor growth in brain, U87MG glioblastoma cells were implanted intracranially into nude mice. Starting 5 days after tumor implantation, mice were treated with CUDC-305 (120 mg/kg, orally, q2d) or vehicle control. As shown in Fig. 3C, treatment with CUDC-305 significantly prolonged survival of intracranial tumor-bearing mice ($P < 0.01$, Mantel-Cox log-rank test).

CUDC-305 causes degradation of oncoproteins and induces tumor regression in the animal models of MV4-11 AML. Our earlier *in vitro* studies showed that CUDC-305 can potently inhibit mutant oncoprotein FLT3 and its downstream signaling molecule STAT5 (Fig. 1C), leading to potent antiproliferative activity

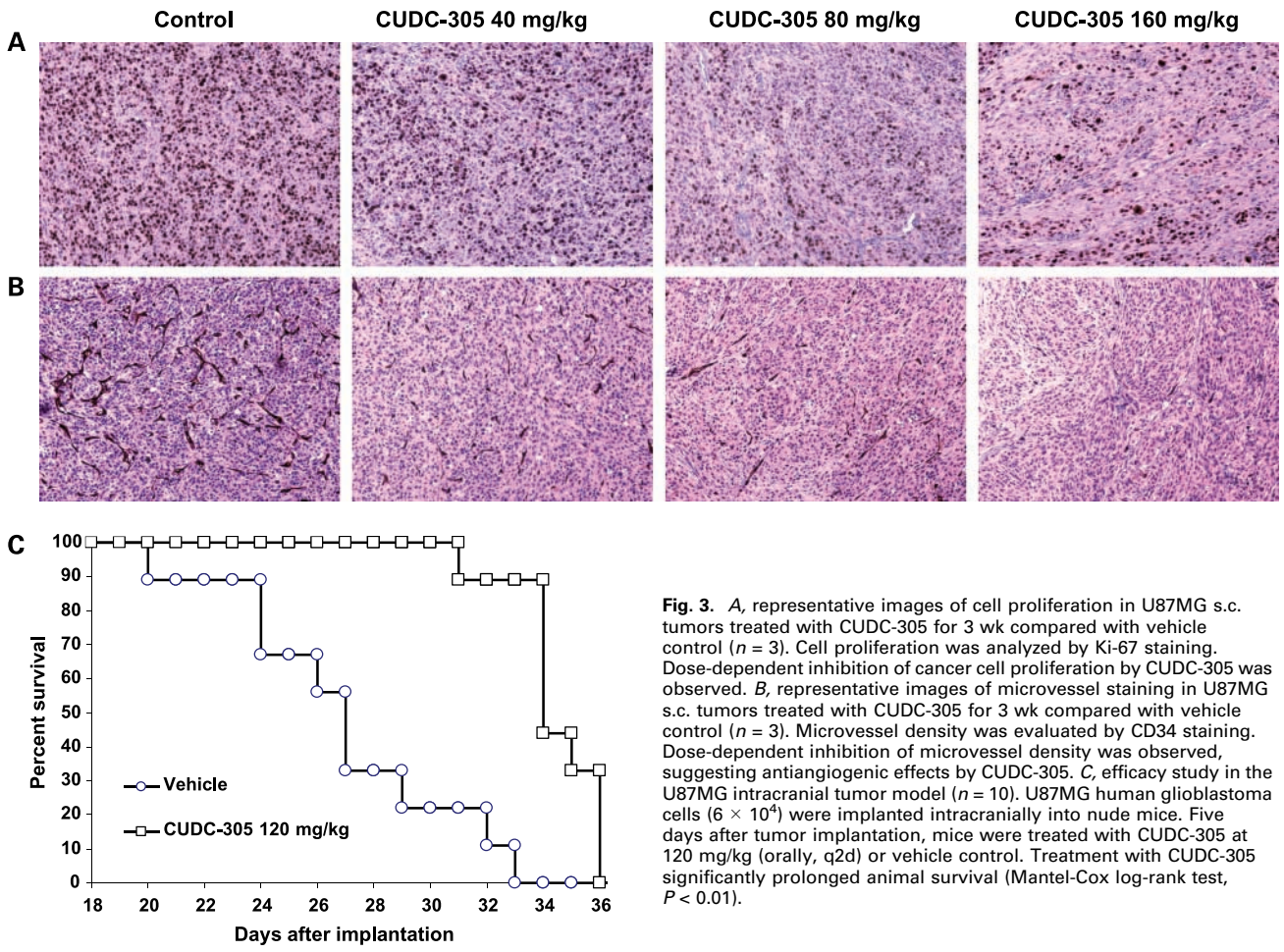

Fig. 3. *A,* representative images of cell proliferation in U87MG s.c. tumors treated with CUDC-305 for 3 wk compared with vehicle control ($n = 3$). Cell proliferation was analyzed by Ki-67 staining. Dose-dependent inhibition of cancer cell proliferation by CUDC-305 was observed. *B,* representative images of microvessel staining in U87MG s.c. tumors treated with CUDC-305 for 3 wk compared with vehicle control ($n = 3$). Microvessel density was evaluated by CD34 staining. Dose-dependent inhibition of microvessel density was observed, suggesting antiangiogenic effects by CUDC-305. *C,* efficacy study in the U87MG intracranial tumor model ($n = 10$). U87MG human glioblastoma cells (6×10^4) were implanted intracranially into nude mice. Five days after tumor implantation, mice were treated with CUDC-305 at 120 mg/kg (orally, q2d) or vehicle control. Treatment with CUDC-305 significantly prolonged animal survival (Mantel-Cox log-rank test, $P < 0.01$).

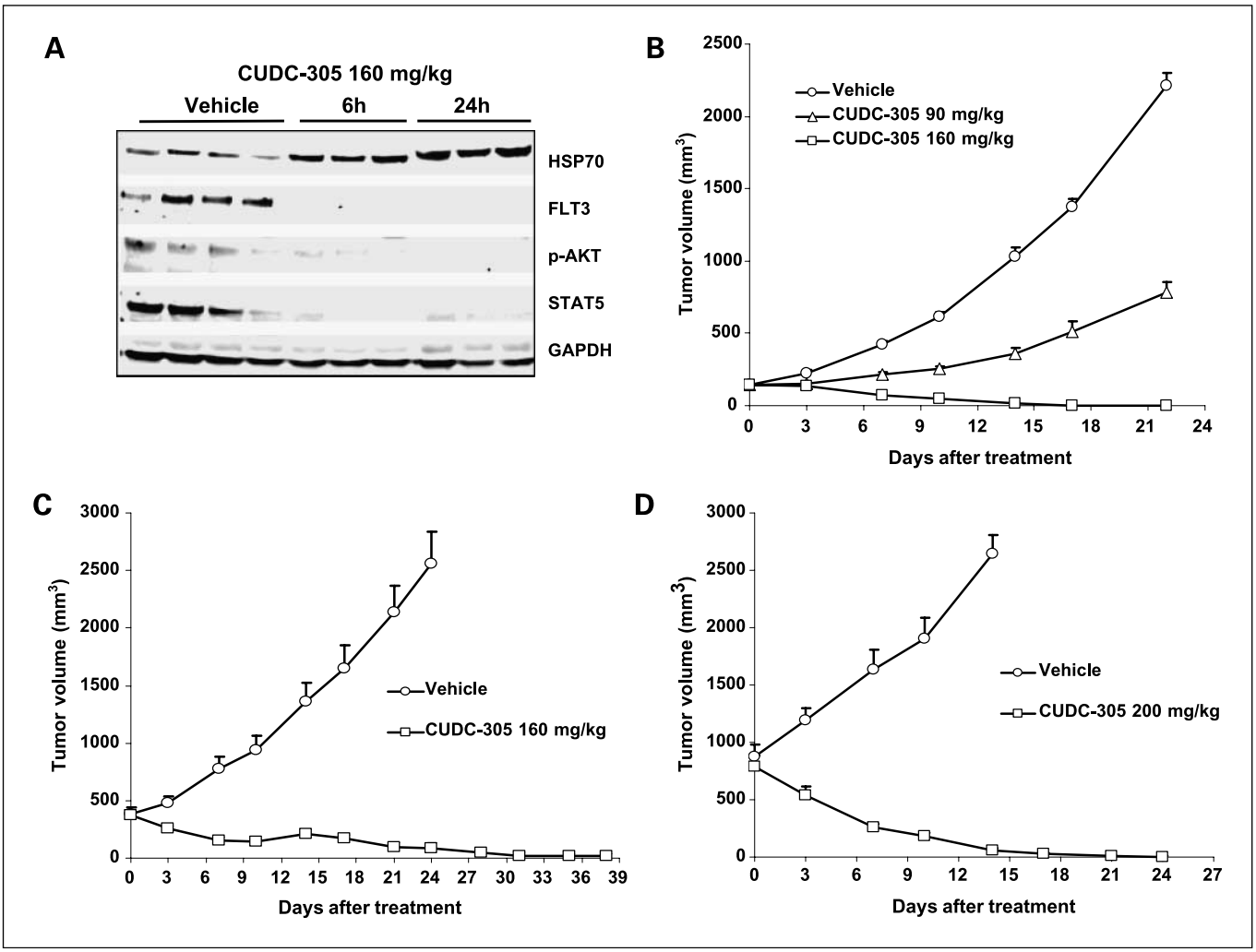

Fig. 4. *A,* PD study after single dosing of CUDC-305 in MV4-11 s.c. tumors. After a single oral dosing of CUDC-305 at 160 mg/kg, tumors were collected at 6 and 24 h ($n = 3$), homogenized, and analyzed by Western blot using antibodies as indicated. Potent inhibition of FLT3 and downstream signaling components p-AKT and STAT5 and induction of HSP70 were observed. *B,* efficacy study of CUDC-305 in the MV4-11 s.c. tumor model ($n = 8$). MV4-11 AML cells (20×10^6) were implanted s.c. into severe combined immunodeficient mice. Treatment with CUDC-305 (160 mg/kg, orally, q2d) started when tumors reached an average volume of 146 mm^3. CUDC-305 treatment for 3 wk induced complete tumor regression ($P < 0.001$). *C* and *D,* efficacy studies ($n = 5$) with larger tumors (pretreatment volume of 380 and 835 mm^3, respectively) in the MV4-11 s.c. tumor models. Complete tumor regression was observed after CUDC-305 treatment at 160 and 200 mg/kg, respectively ($P < 0.001$).

in MV4-11 AML cell line with a low IC_{50} (100 nmol/L; Table 1). Based on these results, we decided to further evaluate the antitumor efficacy of CUDC-305 in MV4-11 tumor xenografts implanted s.c. into severe combined immunodeficient mice. A single-dose PD study was first conducted to evaluate the biological effects of the compound *in vivo*. As shown in Fig. 4A, a single oral dosing (160 mg/kg) of CUDC-305 was able to down-regulate mutant FLT3 and downstream signaling molecules p-AKT and STAT5 with concurrent induction of HSP70. In the same tumor xenograft model, a 3-week treatment with CUDC-305 (160 mg/kg, orally, q2d) induced complete tumor regression ($P < 0.001$) in mice with small-sized pretreatment tumors (146 mm^3), whereas tumors in the control group grew exponentially, reaching 2,200 mm^3 by the end of study (Fig. 4B). However, CUDC-305 delivered on a different dosing schedule (90 mg/kg, 2-1-2, on-off-on) was much less efficacious. Furthermore, CUDC-305 treatment at 160 and 200 mg/kg (orally, q2d) induced complete tumor regression in mice with large-sized pretreatment tumors (380 and 835 mm^3, respectively, $P < 0.001$; Fig. 4C and D). Thus, CUDC-305 is able to induce degradation of both mutant transforming oncoprotein FLT3 and downstream signaling mediators of the FLT3 signaling cascade in the MV4-11 AML model, leading to complete tumor regression.

CUDC-305 induces degradation of multiple signaling proteins and inhibits growth of a NSCLC tumor xenograft resistant to EGFR inhibitor therapy. *In vitro* antiproliferation studies revealed that H1975 cell line, a type of NSCLC that carries a secondary *EGFR* mutation and is resistant to EGFR inhibitors, is sensitive to CUDC-305 treatment (IC_{50}, 140 nmol/L; Table 1). To further evaluate the activity of the compound *in vivo*, we did a single-dose PD study (80 mg/kg, orally) in established H1975 s.c. tumors. As shown in Fig. 5A, we observed potent inhibition of multiple HSP90 client proteins, including mutant EGFR and downstream key regulators of the cell proliferation (c-RAF, p-MEK, phosphorylated ERK), survival (AKT, p-AKT),

and cell cycle progression (CDK4) pathways, as well as increase of HSP70 and induction of apoptosis as measured by poly (ADP-ribose) polymerase cleavage at 8 hours after CUDC-305 treatment (Fig. 5A).

An efficacy study in the same H1975 s.c. tumor model was conducted next. As shown in Fig. 5B, CUDC-305 treatment significantly inhibited H1975 s.c. tumor growth, with a T/C value of 15.4% compared with the control group ($P < 0.001$).

CUDC-305 alone or in combination with standard-of-care agents inhibits tumor growth in other cancer types. In addition to the cancer types described above, CUDC-305 also displayed antitumor efficacy in animal models of various other tumor types. Of particular interest is its shown efficacy in the N87, a HER2 overexpressing gastric tumor model. At a daily dosing of 80 mg/kg, CUDC-305 caused depletion of HER2 protein in tumors analyzed by Western blot and induced tumor regression by 11.3% ($P < 0.001$; data not shown) in the N87 s.c. tumor model. In the MDA-MB-468 breast cancer orthotopic model, potent antitumor activity was also observed. This model belongs to the triple-negative breast cancer subtype, which accounts for 15% of all breast cancers with poor prognoses. When delivered as a single agent at 120 mg/kg for 2 weeks,

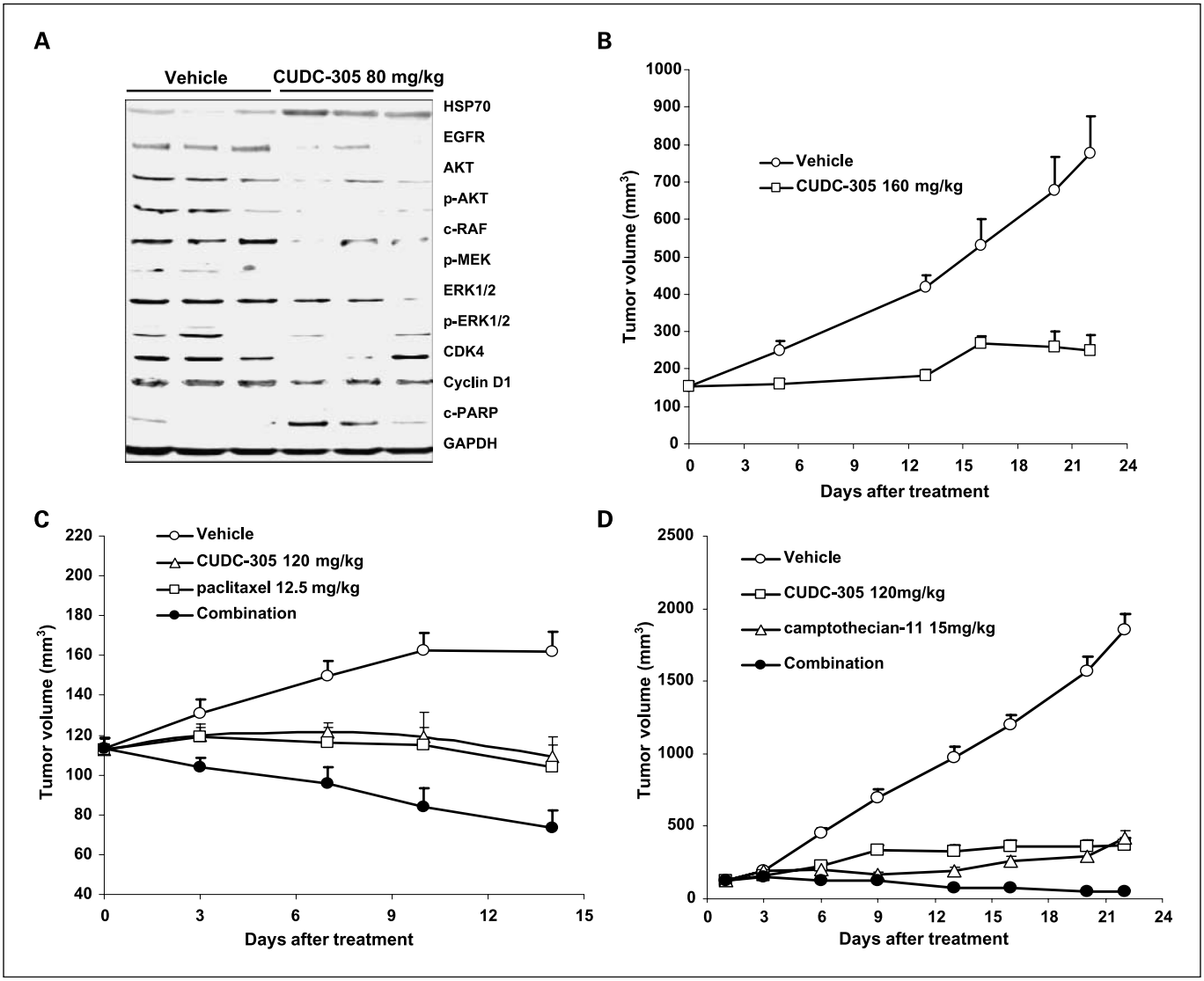

Fig. 5. *A,* PD study after single oral dosing of CUDC-305 in H1975 s.c. tumors. After a single oral dosing of CUDC-305 at 80 mg/kg, tumors were collected at 8 h ($n = 3$), homogenized, and analyzed by Western blot using antibodies as indicated. EGFR and multiple signaling molecules were inhibited. *B,* efficacy study in the H1975 s.c. tumor model ($n = 9$). H1975 NSCLC cells (5×10^6) were implanted s.c. into nude mice. Treatment with CUDC-305 (160 mg/kg, orally, q2d) started when tumors reached an average volume of 160 mm^3. Dosing of CUDC-305 for 3 wk significantly inhibited tumor growth compared with vehicle control (T/C, 15.4%; $P < 0.001$). *C,* efficacy study in the MDA-MB-468 orthotopic tumor model ($n = 8$). MDA-MB-468 breast cancer cells (20×10^6) were implanted orthotopically into nude mice. Treatment started when tumor size reached an average volume of 113 mm^3. CUDC-305 was dosed at 120 mg/kg orally q2d; paclitaxel was dosed at 12.5 mg/kg i.p. twice weekly. CUDC-305 delivered as a single agent induced tumor regression by 3.4% ($P < 0.001$). An enhanced antitumor effect was observed when CUDC-305 was combined with paclitaxel (tumor regression of 36.6%, $P < 0.001$). *D,* efficacy study in the Colo205 s.c. tumor model ($n = 10$). Colo205 colorectal cancer cells (5×10^6) were implanted s.c. into nude mice. Treatment with CUDC-305 started when tumors reached an average volume of 120 mm^3. CUDC-305 was dosed at 120 mg/kg orally q2d. Camptothecin-11 was dosed at 15 mg/kg i.p. twice weekly. CUDC-305 delivered as single agent significantly inhibited tumor growth (T/C, 14.2%; $P < 0.001$). However, an enhanced antitumor activity was observed in the group treated with CUDC-305 and Camptothecin-11 combination ($P < 0.05$).

CUDC-305 induced 3.4% tumor regression ($P < 0.001$; Fig. 5C). In combination with paclitaxel, a standard-of-care agent in breast cancer, CUDC-305 significantly enhanced the antitumor activity of paclitaxel (tumor regression of 36.6%, $P < 0.001$; Fig. 5C). A combination study was also conducted in animal model of Colo205 colorectal cancer, revealing that CUDC-305 significantly enhanced the antitumor activity of camptothecin-11, standard-of-care agent for colorectal cancer therapy ($P < 0.05$; Fig. 5D).

Discussion

Our results show that CUDC-305 is a potent HSP90 inhibitor with optimal pharmacologic properties, including high oral bioavailability, sustained tumor retention, and a potentially favorable therapeutic window. Moreover, its HSP90 binding activity is similar to those of other leading synthetic HSP90 inhibitors.

Pharmacokinetic studies in mice show that CUDC-305 has high oral bioavailability (96.0%), making chronic oral dosing possible. This may represent a differentiating factor compared with other synthetic HSP90 inhibitors, including compounds in the isoxazole class, which have limited bioavailability (21).

Notably, CUDC-305 exhibits a sustained exposure in tumor tissues (Fig. 2A). This favorable pharmacologic property is in contrast to the isoxazole class compounds, which have a reported tumor/plasma AUC ratio of 4.0 after i.v. administration (21), and the purine class compounds, which have shorter half-lives (27).

The selective retention of CUDC-305 in tumor tissues can be attributed to a few factors. First, HSP90 is likely overexpressed in cancer cells to support cancer cell transformation. Increased HSP90 expression in cancer cells has also been described as a stress response to gene mutations and metabolic dysregulation, as well as to hostile environmental conditions including hypoxia, nutrient deprivation, and acidosis (28). Second, HSP90 protein isolated from tumor tissues seems to have an enhanced affinity for HSP90 inhibitors. Indeed, it has been reported that tumor-derived HSP90 has a 100-fold higher binding affinity for 17-AAG than does HSP90 from normal cells (29). This may be a result of conformational differences in HSP90 in cancer versus normal cells. In cancer cells, HSP90 exists as an activated superchaperone complex that is hypersensitive to HSP90 inhibition, whereas in normal cells, HSP90 is predominantly uncomplexed and less sensitive to HSP90 inhibition (30, 31). Finally, in contrast to other HSP90 inhibitors in clinical development, CUDC-305 has a relatively high lipophilicity with a cLogP of ~4.0. These balanced chemical properties may facilitate its penetration and retention in tumors. Therefore, the abundance of HSP90 in cancer cells, its high affinity for HSP90 inhibitors, and the high lipophilicity of CUDC-305 all contribute to the selective accumulation and retention of CUDC-305 in tumor tissues. The preferential retention of CUDC-305 in tumors may also explain its selective effects on tumor cells (mean IC_{50}, 220 nmol/L) as opposed to normal human primary cells (mean IC_{50}, ~500 nmol/L) as observed in our in-house antiproliferation studies (data not shown). Isoxazole class compounds, in contrast, were reported to be active against human cancer cells, as well as nontumorigenic human prostate and breast epithelial cells (21). The selective pharmacologic action of CUDC-305 is essential to achieve enhanced efficacy and reduced toxicity *in vivo*.

The sustained exposure of CUDC-305 in tumor cells results in persistent biological effects, as shown in the single-dose PD study in U87MG s.c. tumors (Fig. 2B). These biological effects have been maintained for as long as 48 hours after a single dosing of CUDC-305, supporting the use of an q2d dosing regimen in efficacy studies. A 2-week pharmacokinetic simulation based on single oral dosing of CUDC-305 at 30 and 160 mg/kg shows no accumulation in normal tissues but a sustained exposure and accumulation in tumor tissues (data not shown), providing further evidence for an intermittent dosing schedule. Although nonlinear exposure was observed in tumor tissues for the two dosage levels used, in difference from plasma exposure, which seems roughly dose-proportional, additional dose-linearity studies with more dosage levels of compound will be pursued in future.

Cell-based assays reveal that CUDC-305 potently inhibits the growth of a broad range of cancer cell lines derived from both solid and hematologic tumors (Table 1). Moreover, cancer cells with oncogenic mutations and/or amplifications (*HER2*, *FLT*, *B-RAF*, *c-MET*, etc.) seem to be relatively sensitive to CUDC-305, suggesting that these oncoproteins are highly dependent on HSP90 chaperone function and that CUDC-305 can exploit the "oncogenic addiction" of some cancer cells. The sensitivity of these cancer cell lines to CUDC-305 is consistent with the potent inhibition of oncogenic proteins of the compound and downstream signaling molecules as shown in the *in vitro* mechanism of action studies (Fig. 1B-D).

Due to the inability of many anticancer drugs to effectively penetrate the blood-brain barrier, both primary and metastatic brain cancers represent a crucial unmet medical need. Among synthetic HSP90 inhibitors, CUDC-305 is unique in its high distribution in brain tissue. SNX-5422, for example, reportedly does not reach the brain (22). We first showed in an s.c. tumor model, that CUDC-305 can inhibit U87MG glioblastoma tumor growth in a dose-dependent manner (Fig. 2C). Then we showed that CUDC-305 is able to inhibit intracranial glioblastoma growth and prolong animal survival in an intracranial tumor model (Fig. 3C), supporting its pharmacologic activity via blood-brain barrier penetration. PD studies in U87MG s.c. tumors collected at the end of the efficacy study showed a dose-dependent inhibition of multiple HSP90 client proteins by CUDC-305 (Fig. 2D), correlating with efficacy results. These down-regulated HSP90 client proteins include ones involved in cell proliferation, as well as cell survival. The latter result is particularly noteworthy because the AKT pathway is constitutively activated in U87MG cells due to *PTEN* gene deletions. Roughly one third of glioblastoma patients carry such *PTEN* deletions, a mutation that confers primary resistance to EGFR inhibitors (32). Because EGFR and AKT are both HSP90 client proteins, HSP90 inhibitors may be a more effective therapeutic strategy in glioblastoma than EGFR inhibitors. Considering the poor prognosis of glioblastoma and other brain cancers, as well as the dearth of effective therapeutic agents, the potential of CUDC-305 as an agent for primary and metastatic brain cancers is significant. Although blood-brain barrier penetration may raise concern over central nervous system toxicity, CUDC-305 with a unique chemical structure displays no central nervous

system–related toxicity in our GLP toxicology studies. Nonetheless, central nervous system toxicity will be further evaluated and closely monitored in future studies.

The activity of CUDC-305 in cancer cell lines with gene mutations was further confirmed in the MV4-11 AML tumor xenograft model. CUDC-305 is able to induce complete tumor regression in three separate studies with various pretreatment tumor sizes (Fig. 4B-D). This antitumor effect is associated with a robust inhibition of the transforming mutant oncoprotein FLT3, as well as downstream signaling molecule STAT5, as shown in both *in vitro* (Fig. 1C) and *in vivo* (Fig. 4A). These results may suggest that MV4-11 AML cells have "highjacked" and, thus, become addicted to the hyperactivated FLT3 signaling pathway for survival, which in turn is highly dependent on HSP90 chaperone function for maintenance of the deregulated pathway components. Therefore, complete blockade of FLT3 signaling through simultaneous inhibition of the two key regulators (both FLT3 and STAT5) of the FLT3 signaling pathway by CUDC-305 treatment can abrogate malignant phenotype, leading to fast tumor regression. In humans, the *FLT3* internal tandem duplication mutation causes constitutive, ligand-independent activation of the FLT3 tyrosine kinase, leading to leukemogenesis (33). Moreover, in roughly 20% to 25% of AML cases, this mutation may also contribute to an aggressive malignant phenotype and resistance to traditional therapies (34). Considering the prevalence and lethality of AML and the lack of advances in treatment in the past 35 years, the potent antitumor activity of CUDC-305 in AML as single agent is exciting. An important direction for future study will be to test CUDC-305 activity in AML cell lines with wild-type *FLT3*, an isoform that is overexpressed in 80% of AML cases. In addition to *FLT3* mutation and/or overexpression, it has been recognized that several types of oncogenes underlie AML development. Therefore, it is conceivable that simultaneous inhibition of multiple pathways in the same leukemic cell by CUDC-305 will be a more broadly applicable therapeutic approach than the selective FLT3 inhibitors currently under development (35–38).

Perhaps, most importantly, CUDC-305 displays potent antitumor activity against H1975 NSCLC cancer cell line harboring *EGFR* secondary mutation responsible for acquired erlotonib resistance (Table 1; Fig. 5B). This mutation, *T790M*, enhances EGFR catalytic activity and confers resistance to reversible tyrosine kinase inhibitors (39). Our PD study in H1975 tumor shows that CUDC-305 is able to induce simultaneous degradation of multiple HSP90 client proteins *in vivo*, including mutant EGFR and key regulators of the RAF/MEK/ERK and PI3K/AKT signaling cascades downstream of EGFR (Fig. 5A). In addition, CUDC-305 exhibits activity both *in vitro* (Table 1) and *in vivo* (data not shown) against NSCLC cell lines that carry either *K-ras* mutations (Calu-6, H460) or *c-MET* amplification (H1993), genetic abnormalities thought to confer primary resistance to erlotinib. *K-ras* mutations constitutively activate downstream RAF/MEK/ERK signaling independent of upstream EGFR inhibition, conferring primary resistance to EGFR inhibitors (40). The activity of the compound in *K-ras* mutant NSCLC cell lines may be due to its ability to inhibit multiple signaling pathways, such as AKT and MAPK/ERK downstream of RAS. In light of these results, it seems reasonable to expect that targeting HSP90 may be a more efficacious approach in overcoming both primary and acquired resistance in NSCLC than the irreversible EGFR inhibitors, which caused incomplete blockade of the AKT signaling in *T790M*-driven tumors (41), offering the potential for significant therapeutic benefits.

MDA-MB-468, a breast cancer cell line, is resistant to the HSP90 inhibitor 17-AAG due to a mutation in the *NQO1* gene, which encodes DT-Diaphorase, an enzyme that metabolizes 17-AAG to a more potent form, 17-AAGH2 (42). However, CUDC-305 showed potent antitumor activity in this cell line *in vitro* (Table 1) as well as *in vivo* (Fig. 5C), suggesting that CUDC-305 inhibits tumor growth independently of *NQO1* status and may have a broader spectrum of activity than 17-AAG. An important area for future study is the mechanism of CUDC-305 sensitivity in the triple-negative breast cancer subtype, a particularly devastating form for which effective therapeutics are sorely lacking. In MDA-MD-468 breast cancer and Colo205 colorectal cancer models, we show that CUDC-305 can enhance the antitumor activity of standard-of-care agents (Fig. 5C and D), an effect that is likely due to AKT suppression as a result of HSP90 inhibition (43).

In summary, CUDC-305 is a novel, synthetic, small-molecule inhibitor of HSP90 with potent and sustainable biological effects in cancer as shown *in vitro* and *in vivo*. Its antitumor effect likely stems from its ability to simultaneously block multiple signaling pathways, effectively interrupting the interactions among signaling networks in cancer cells. In addition, it displays other optimal pharmacologic properties, including high oral bioavailability, sustained tumor retention, blood-brain barrier penetration, and a potentially more favorable therapeutic window. Furthermore, *in vitro* safety and toxicology studies suggest a favorable safety profile. Based on these results, CUDC-305 has been nominated as a drug candidate for further development.

Disclosure of Potential Conflicts of Interest

All authors are employees and shareholders of Curis, Inc.

Acknowledgments

We thank Crown Bioscience, Inc., for conducting efficacy studies in the U87MG glioblastoma intracranial model and Colo205 colorectal tumor xenograft model, Ricky Sanchez for preparing tissue sections for histologic analyses, Carmen Pepicelli and Mitchell Keegan of Curis Drug Development group for helpful discussion, and Nicole Davis for assistance in preparation of this manuscript.

References

1. Croce CM. Oncogenes and cancer. N Engl J Med 2008;358:502–11.
2. Nadal E, Olavarria E. Imatinib mesylate (Gleevec/Glivec) a molecular-targeted therapy for chronic myeloid leukaemia and other malignancies. Int J Clin Prac 2004;58:511–6.
3. Cavazos JMS, Guerrero JFG, Villanueva WOB, Mestres JA, Torres JMB. Trastuzumab (Herceptin) in the treatment of breast cancer with HER2 overexpression. Clin Trans Oncol 2001;3:172–82.
4. Riely GJ. The use of first-generation tyrosine kinase inhibitors in patients with NSCLC and somatic EGFR mutations. Lung Cancer 2008;60:S19–22.
5. Velcheti V, Viswanathan A, Ramaswamy G. The proportion of patients with metastatic non-small cell lung cancer potentially eligible for treatment with bevacizumab: a single institutional survey. J Thoracic Oncol 2006;1:501.
6. Workman P, Burrows F, Neckers L, Rosen N. Drugging the cancer chaperone HSP90:

combinatorial therapeutic exploitation of oncogene addiction and tumor stress. Ann N Y Acad Sci 2007;1113:202–16.

7. Lu Y, Zi X, Zhao Y, Mascarenhas D, Pollak M. Insulin-like growth factor-I receptor signaling and resistance to trastuzumab (Herceptin). J Natl Cancer Inst 2001;93:1852–7.

8. Engelman JA, Zejnullahu K, Mitsudomi T, et al. MET amplification leads to gefitinib resistance in lung cancer by activating ERBB3 signaling. Science 2007;316:1039–43.

9. Pao W, Miller VA, Politi KA, et al. Acquired resistance of lung adenocarcinomas to gefitinib or erlotinib is associated with a second mutation in the EGFR kinase domain. PLoS Med 2005;2:225–35.

10. Engelman JA, Jänne PA, Mermel C. ErbB-3 mediates phosphoinositide 3-kinase activity in gefitinib-sensitive non-small cell lung cancer cell lines. Proc Natl Acad Sci U S A 2005;102:3788–93.

11. Maloney A, Workman P. HSP90 as a new therapeutic target for cancer therapy: the story unfolds. Expert Opin Biol Ther 2002;2:3–24.

12. Kamal A, Boehm MF, Burrows FJ. Therapeutic and diagnostic implications of Hsp90 activation. Trends Mol Med 2004;10:283–90.

13. Chiosis G, Vilenchik M, Kim J, Solit D. Hsp90: the vulnerable chaperone. Drug Discovery Today 2004;9:881–8.

14. Mosser DD, Morimoto RI. Molecular chaperones and the stress of oncogenesis. Oncogene 2004;23:2907–18.

15. Obermann WM, Sondermann H, Pavletich NP, Hartl FU. *In vivo* function of Hsp90 is dependent on ATP binding and ATP hydrolysis. J Cell Biol 1998;143:901–10.

16. Modi S, Sugarman S, Stopeck A, et al. Phase II trial of the Hsp90 inhibitor tanespimycin (Tan) + trastuzumab (T) in patients (pts) with HER2-positive metastatic breast cancer (MBC). J Clin Oncol 2008;26:2008 sul abstr 1027.

17. Vilenchik M, Solit D, Basso A, et al. Targeting wide-range oncogenic transformation via PU24FCl, a specific inhibitor of tumor Hsp90. Chem Biol 2004;11:787–97.

18. Powers MV, Workman P. Targeting of multiple signaling pathways by heat shock protein 90 molecular chaperone inhibitors. Endocrine-Related Cancer 2006;13:S125–35.

19. Banerji U, Judson I, Workman P. The clinical applications of heat shock protein inhibitors in cancer - present and future. Curr Cancer Drug Targets 2003;3:385–90.

20. Chiosis G, Lucas B, Huezo H, Solit D, Basso A, Rosen N. Development of purine-scaffold small molecule inhibitors of Hsp90. Curr Cancer Drug Targets 2003;3:371–6.

21. Eccles SA, Massey A, Raynaud FI, et al. NVP-AUY922:A novel heat shock protein 90 inhibitor active against xenograft tumor growth, angiogenesis, and metastasis. Cancer Res 2008;68:2850–60.

22. Chandarlapaty S, Sawai A, Ye Q, et al. SNX2112, a synthetic heat sock protein 90 inhibitor, has potent antitumor activity against HER kinase dependent cancers. Clin Cancer Res 2008;14:240–8.

23. Bao R, Selvakumaran M, Hamilton TC. Use of a surrogate marker (human secreted alkaline phosphatase) to monitor *in vivo* tumor growth and anticancer drug efficacy in ovarian cancer xenografts. Gynecol Oncol 2000;78:373–9.

24. Alley MC, Hollingshead MG, Dykes DJ, Waud WR. Human tumor xenograft models in NCI drug development. In: Teicher BA, Andrews PA, editors. Anticancer drug development guide. New Jersey: Humana Press, Inc.; 2004, p. 125–52.

25. Cai X, Qian C, Zhai H, inventors; Curis Inc., assignee. Fused amino-pyridine as HSP90 inhibitors. World Intellectual Property Organization WO 2008/115719 A1. 2008 Sept 25.

26. Xia W, Bacus S, Hegde P. A model of acquired autoresistance to a potent ErbB2 tyrosine kinase inhibitor and a therapeutic strategy to prevent its onset in breast cancer. Proc Natl Acad Sci U S A 2006;103:7795–800.

27. Elfiky A, Saif MW, Beeram M, et al. BIIB021, an oral, synthetic non-ansamycin Hsp90 inhibitor: phase 1 experience. J Clin Oncol 2008;26 suppl:abstr 2503.

28. Ferrarini M, Heltai S, Zocchi MR, Rugarli C. Unusual expression and localization of heat-shock proteins in human tumor cells. Int J Cancer 1992;51:613–9.

29. McCarthy MM, Pick E, Kluger Y, et al. HSP90 as a marker of progression in melanoma. Ann Oncol 2007;19:590–4.

30. Chiosis G, Neckers L. Tumor selectivity of Hsp90 inhibitors-the explanation remains elusive. ACS Chem Biol 2006;1:279–84.

31. Kamal A, Thao L, Sensintaffar J, et al. A high-affinity conformation of Hsp90 confers tumour selectivity on Hsp90 inhibitors. Nature 2003;425:407–10.

32. Gonzalez J, Groot JD. Combination therapy for malignant glioma based on PTEN status. Expert Rev Anticancer Ther 2008;8:1767–79.

33. Nakao M, Yokota S, Iwai T, et al. Internal tandem duplication of the flt3 gene found in acute myeloid leukemia. Leukemia 1996;10:1911–8.

34. Levis M, Allebach J, Tse KF. A FLT3-targeted tyrosine kinase inhibitor is cytotoxic to leukemia cells *in vitro* and *in vivo*. Blood 2002;99:3885–91.

35. Yee KW, O'Farrell AM, Smolich BD. SU5416 and SU5614 inhibit kinase activity of wild-type and mutant FLT3 receptor tyrosine kinase. Blood 2002;100:941–9.

36. O'Farrell AM, Abrams TJ, Yuen HA, et al. SU11248 is a novel FLT3 tyrosine kinase inhibitor with potent activity *in vitro* and *in vivo*. Blood 2003;101:3597–605.

37. Mesters RM, Padro T, Bieker R, et al. Stable remission after administration of the receptor tyrosine kinase inhibitor SU5416 in a patient with refractory acute myeloid leukemia. Blood 2001;98:241–3.

38. Kelly LM, Yu JC, Boulton CL, et al. CT53518, a novel selective FLT3 antagonist for the treatment of acute myelogenous leukemia (AML). Cancer Cell 2002;1:21–32.

39. Shimamura T, Li D, Ji H, et al. Hsp90 inhibition suppresses mutant EGFR-T790M signaling and overcomes kinase inhibitor resistance. Cancer Res 2008;68:5827–38.

40. Massarelli E, Varella-Garcia M, Tang X, et al. KRAS mutation is an important predictor of resistance to therapy with epidermal growth factor receptor tyrosine kinase inhibitors in non-small-cell lung cancer. Clin Cancer Res 2007;13:2890–6.

41. Shimamura T, Lowell AM, Engelman JA, Shapiro GI. Epidermal growth factor receptors harboring kinase domain mutations associate with the heat shock protein 90 chaperone and are destabilized following exposure to geldanamycins. Cancer Res 2005;64:6401–8.

42. Guo W, Reigan P, Siegel D, Zirrolli J, Gustafson D, Ross D. Formation of 17-allylamino-demethoxygeldanamycin (17-AAG) hydroquinone by NAD(P)H:quinone oxidoreductase 1: role of 17-AAG hydroquinone in heat shock protein 90 inhibition. Cancer Res 2005;65:10006–15.

43. Münster PN, Basso A, Solit D. Modulation of Hsp90 function by ansamycins sensitizes breast cancer cells to chemotherapy-induced apoptosis in an RB- and schedule-dependent manner: see the biology behind: E. A. Sausville, combining cytotoxics and 17-allylamino, 17-demethoxygeldanamycin:sequence and tumor biology matters. Clin Cancer Res 2001;7:2155–8.

Clinical Cancer Research

CUDC-305, a Novel Synthetic HSP90 Inhibitor with Unique Pharmacologic Properties for Cancer Therapy

Rudi Bao, Cheng-Jung Lai, Hui Qu, et al.

Clin Cancer Res 2009;15:4046-4057.